Journal of Physics and Chemistry of Solids 153 (2021) 109991

Contents lists available at ScienceDirect

Journal of Physics and Chemistry of Solids

journal homepage: http://www.elsevier.com/locate/jpcs

Amorphous zircon at high pressure

Süleyman Bolat [a], Murat Durandurdu [b,*]

[a] Faculty of Science, Department of Physics, Karadeniz Technical University, Trabzon, 61080, Turkey
[b] Nanotechnology Engineering, Abdullah Gül University, Kayseri, 38080, Turkey

ARTICLE INFO

Keywords:
Amorphous
$ZrSiO_4$
High pressure

ABSTRACT

The high-pressure behavior of a very low-density amorphous zircon model having Zr (Si) coordination of 5.6 (4.02) is explored by ab initio simulations. Two consecutive pressure-induced phase modifications are proposed for this material. The first transition is from a very low-density amorphous state to a dense amorphous state having Zr (Si) coordination of 7.3 (4.5). The second one is from the dense phase to a high-density amorphous structure with Zr and Si coordination numbers of about 8 and 5.5, correspondingly. Both phase changes proceed progressively. The first phase transformation is irreversible whist the second one is reversible.

The Voronoi polyhedron analysis reveals the presence of polyhedron of the zircon crystal (<0,4,4,0>), the zirconia baddaliyette phase (<1,3,3,0>) and the zirconia cotunnite state (<0,3,6,0>) around Zr atoms in the amorphous states formed on both compression and decompression, meaning that the amorphous configurations consist of a mixed state of them.

1. Introduction

Zircon ($ZrSiO_4$) is an interesting mineral and demonstrates some remarkable properties such as a high melting point [1,2], high hardness [3], high thermal conductivity and chemical stability [4]. Researchers have focused on this material for last decades due to its potential applications. Namely, it can be used in jewelry industry, electronic sectors as a dielectric material, nuclear industry and laser technology [5–8].

Zircon with space group $I4_1/amd$ has the lattice constants of $a = b =$ 6.607 Å and $c = 5.981$ Å, and its structural orientation is orthosilicate with the tetragonal symmetry. Zr^{4+} and Si^{4+} cations having $\bar{4}2m$ symmetry form ZrO_8 polyhedrons and SiO_4 tetrahedral structures [9,10]. The tetragonal zircon converts to a scheelite-structure (space group $I4_1/a$, $a = b = 4.738$ Å and $c = 10.51$ Å) at high temperature and/or pressure conditions. Owing to this phase modification, its density rises approximately 10% [11].

Natural amorphous zircon is a result of radiation damage over years. It consists of both noncrystalline and crystalline domains and thus it is termed metamict zircon. Its local structure strongly depends on the radiation time and dose [12]. At laboratory conditions, amorphization of zircon can be also reachable using the reactive magnetron sputtering technique, heavy ions methods and sol-gel processing but as in natural case, full amorphization could not be realized [13–15]. It appears that the rapid solidification technique is ineffective in yielding an amorphous state of zircon [16].

The high pressure behavior of the radiation amorphized zircon was experimentally investigated up to 9 GPa and a gradual phase change into a high density amorphous (HDA) arrangement was reported [17]. This phase transformation is irreversible. In the same work, ab initio molecular dynamics (MD) simulations were also executed to have an atomistic level picture of the structural modifications under pressure and it was disclosed that the densification of amorphous zircon is associated with a coordination increase of Zr atoms from about 7 to 8. Furthermore, the presence of a very high density amorphous (VHDA) form of zircon at higher pressures was proposed in the simulations [17]. Another experimental study on metamict zircon also suggested structural changes between ~3 and 6 GPa and the irreversibility of the phase transformation [18].

Recently we have reported the existence of a very low-density amorphous form of zircon based on the quantum mechanical simulations [19]. The coordination number of Zr and Si atoms in this noncrystalline arrangement is estimated to be about 5.66 and 4.0, correspondingly. The main purpose of the present study is to probe its high-pressure behavior in details and to compare our findings with those of Ref. [17].

* Corresponding author.
E-mail address: murat.durandurdu@agu.edu.tr (M. Durandurdu).

https://doi.org/10.1016/j.jpcs.2021.109991
Received 15 April 2020; Received in revised form 2 February 2021; Accepted 3 February 2021
Available online 6 February 2021

Table 1
The lattice parameters and the atomic positions of crystalline zircon.

Lattice parameters	present	Ref. [10][exp.]
a (Å)	6.660	6.604
c (Å)	6.067	5.980
Fractional Positions		
Zr (4*a*)		
x	0.0000	0.0000
y	0.7500	0.7500
z	0.1250	0.1250
Si (4*b*)		
x	0.0000	0.0000
y	0.7500	0.7500
z	0.6250	0.6250
O (16*h*)		
x	0.0000	0.0000
y	0.0647	0.0660
z	0.1940	0.1951

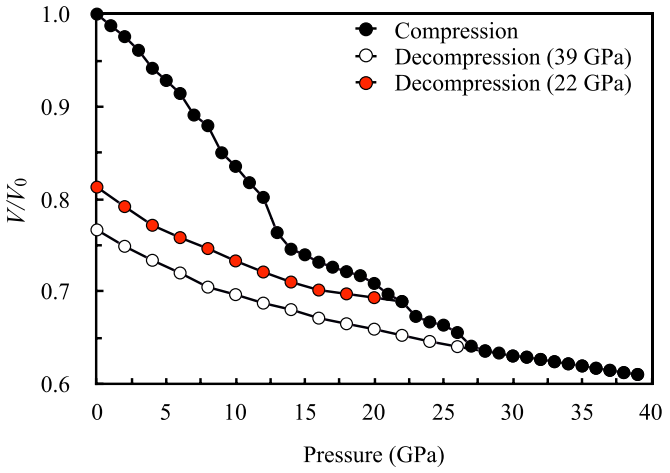

Fig. 1. Pressure-volume relation of amorphous zircon under compression and decompression.

2. Methodology

The ab initio MD investigation was achieved by the SIESTA code [20]. The pseudopotentials were produced using the Troullier-Martins approach [21]. The PBE generalized gradient approximation (GGA) was preferred [22] for the exchange correlation term. The extensive DZP orbitals were selected. The electronic structure of the systems was determined by the standard diagonalization method. The simulation parameters selected were first tested for the crystal and our results along with experimental data were summarized in Table 1, demonstrating that the parameters used in the present study were reliable enough to model an amorphous structure and to study its high-pressure behavior. In our earlier work [19], we generated an amorphous zircon configuration having 192 atoms using the usual melt and quench technique and a cooling rate of 3.6×10^{13} K/ps (see Ref. [19] for more information). The lattice parameters of the amorphous structure are $a = 13.631$ Å, $b = 15.503$ Å, $c = 13.030$ Å, $\alpha = 90.39°$, $\beta = 89.08°$ and $\gamma = 90.39°$, and corresponding density is 3.54 g/cm^3. This density is significantly less than 4.52 g/cm^3 estimated for the crystal and 3.7–4.9 g/cm^3 of metamict zircon [23] and hence this amorphous structure is referred as a low-density amorphous zircon. In the present study, we extended our study and investigated its response to pressure. The simulations were accomplished within the isoenthalpic-isobaric (NPH) ensemble. The constant pressure relaxation of the atomic structure and volume was attained using the Parrinello-Rahman [24] and the power quenching techniques. The second method sets the velocity components of atoms and simulation cell's parameters zero once the velocities and forces have reverse signs. Our prior researches suggested that the combination of these approaches was quite successful in reproducing/predicting solid-to-solid phase changes in a wide range of amorphous and crystalline materials including amorphous and crystalline zirconia [25,26]. For amorphous zircon, the external pressure was progressively increased up to 39 GPa with an increment of 1.0 GPa. After a certain invariance for the average coordination of the Zr atom was experienced, the pressure applied was gradually reduced to zero in 2 GPa steps.

3. Results

The pressure-volume relation upon the compression and decompression procedures is shown in Fig. 1. With the application of pressure, the volume decreases progressively but the decrease is not smooth. At some pressures, it shows some ripples, and it is possibly related to the small size of the system simulated. Above 27 GPa, the change in the volume develops smoothly, which might an indication of completion of structural modifications induced by the external pressure. On the other hand, upon pressure release from two different pressures of 39 and 22 GPa, the volume slowly increases without any ripples but the original volume is not recovered, demonstrating the existence of an irreversible process and the permanent densification in amorphous zircon, similar to what has been proposed in Refs. [17,18]. The recovered structures are distinctively denser (~19% and ~24% upon decompression from 22 GPa to 39 GPa, respectively) than the uncompressed one.

The pressure-induced structural alterations at the atomistic level are initially explored by partial pair distribution functions (PPDFs). Cation-anion and cation-cation PPDFs of the amorphous zircon model for the chosen external pressures are illustrated in Fig. 2 and Fig. 3, respectively. The structure remains amorphous as indicted by the presence of only short-range order at the highest pressure of 39 GPa applied in this study. This observation can be interpreted as the existence of amorphous-to-amorphous phase transformation(s) in zircon under pressure.

In the next step, we focus on the influence of pressure on the first peak of the PPDFs. The Zr–O bond length is 2.00 Å at ambient pressure, which is, however, less than the previously reported value of 2.07 Å for the amorphous zircon and 2.13 Å for the metamict zircon [27]. With the application of pressure, this bond length increases gradually to 2.07–2.11 Å. Such an increase is undoubtedly associated with the formation of new bonds (coordination) under pressure. During the decompression processes, the Zr–O bond separation enlarges steadily and reaches 2.15 Å at zero pressure. It should be underlined here that these values are reasonably comparable with 2.15 Å in the zircon crystal [19] and 2.13 Å in the metamict zircon [27]. The mean Si–O bond distance of the uncompressed model is 1.65 Å that is in good agreement with experimental value of 1.68 Å in amorphous and liquid zircon [27]. With increasing pressure, this bond separation progressively increases to a value of 1.70 Å at 27 GPa and remains null thereafter. Upon the decompression procedures, it slightly increases and has a value of 1.71 Å at ambient pressure. The Zr–Zr pair splits and the first and second peaks are located at 3.48 Å and at 3.95 Å respectively. These correlation distances are somewhat different from 3.40 Å and 3.90 Å reported in the earlier MD investigation [15]. The splitting is associated with corner (first peak) and edge (second peak) sharing of ZrO_x polyhedrons [15, 28]. So, in the uncompressed model, the edge sharing units are

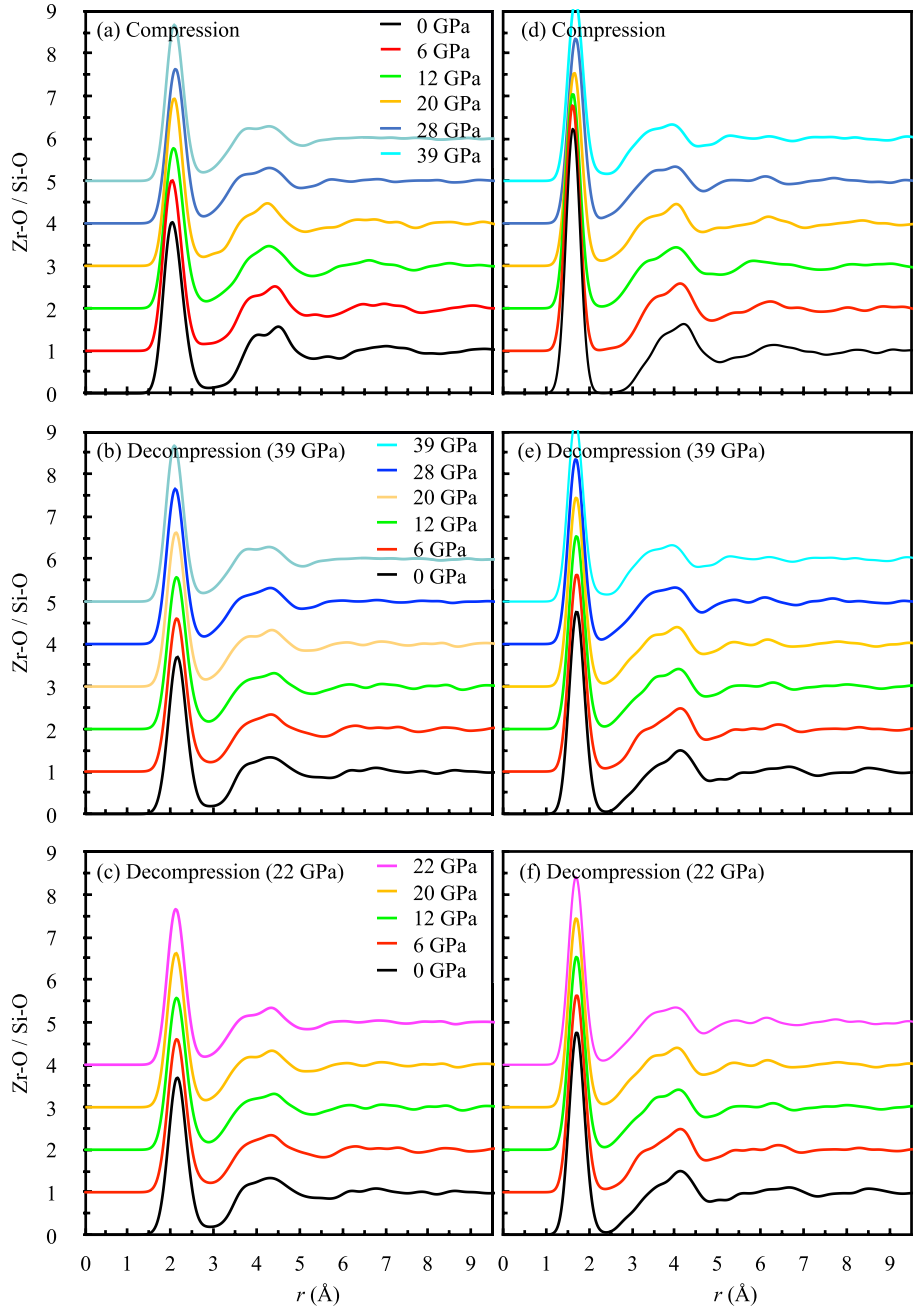

Fig. 2. Cation-anion partial pair distribution functions (PPDFs) of the amorphous zircon model at sellected pressures.

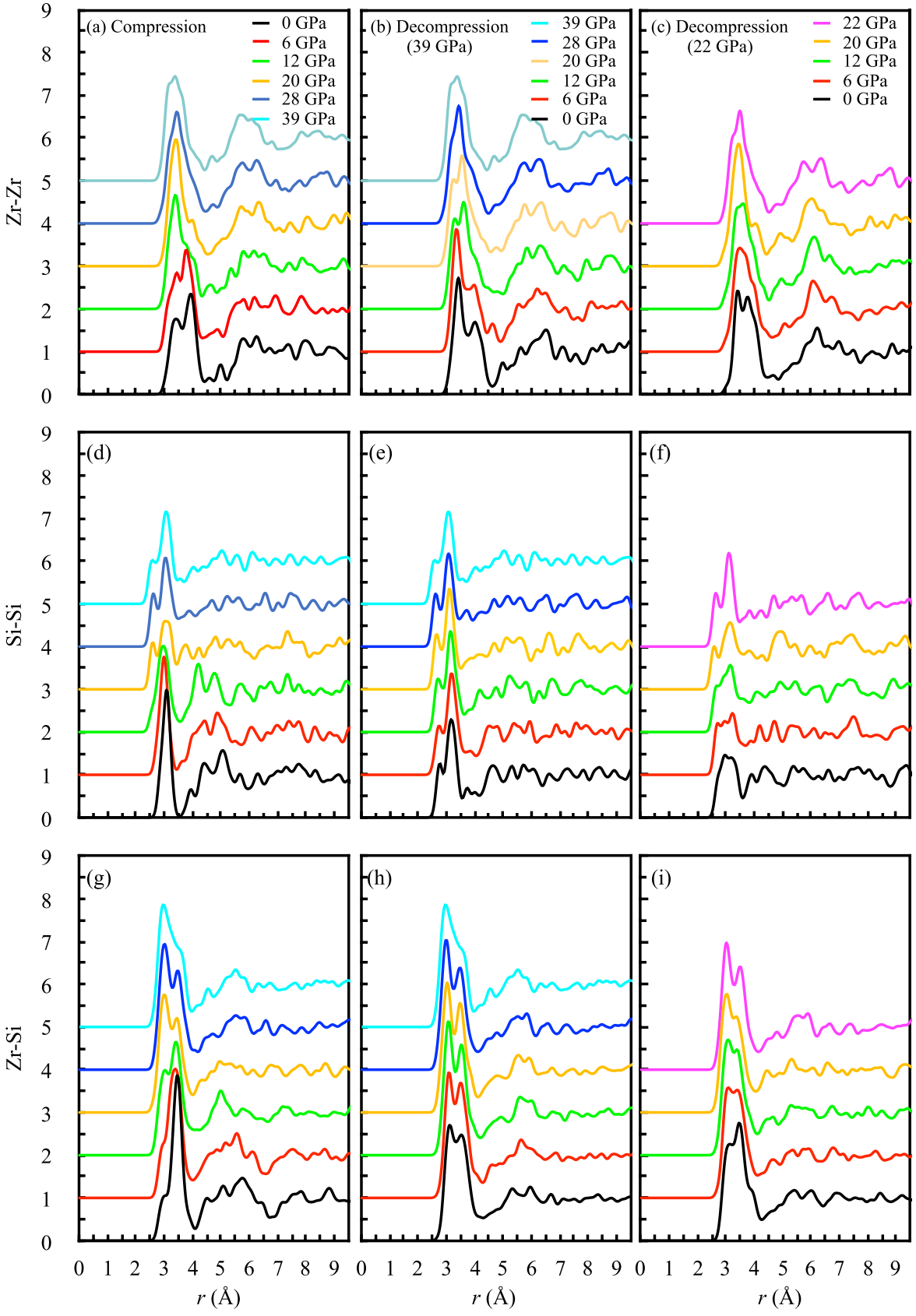

Fig. 3. Cation-cation partial pair distribution functions (PPDFs) of the amorphous zircon model at sellected pressures.

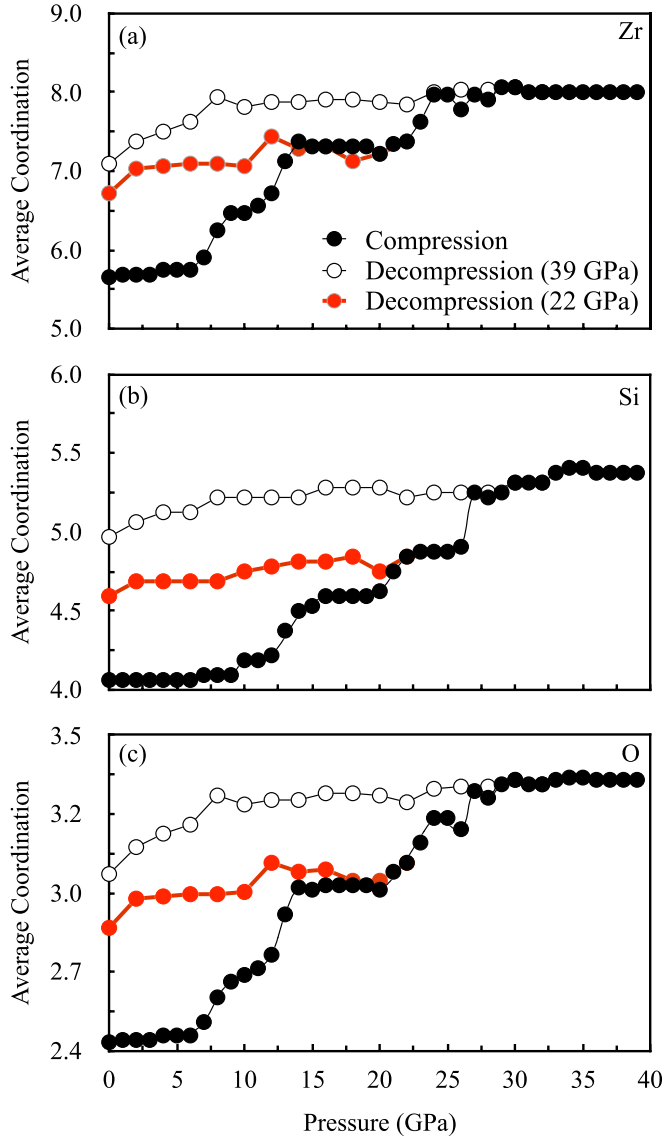

Fig. 4. Modification of the average coordination of Zr, Si and O atoms on compression and decompression processes.

dominated. As the pressure applied is increased, the spitting disappears at 12 GPa. On decompression from 39 GPa, we notice the appearance of the splitting again at 20 GPa while it occurs at 2 GPa upon pressure release from 22 GPa. For the recovered models, however, the first peak becomes more dominant than the second one, implying that they have more corner sharing units than the uncompressed network. The Si–Si separation is located at 3.09 Å in agreement with 3.10–3.13 Å estimated in the earlier studies [15,27]. At 20 GPa, a splitting of the first shell is observed in this correlation and it is preserved upon pressure release. At zero pressure, the first and the second peaks are placed at 2.76 Å and 3.17 Å, correspondingly. The Zr–Si correlation has a shoulder at 3.03 Å and a main peak at 3.65 Å, which are a result of the edge sharing and corner sharing SiO_4 and ZrO_8 units, correspondingly [19]. With increasing pressure, the shoulder becomes the main peak at 12 GPa and remains unchanged on decompression.

The pressure-induced structural modifications are usually recognized by the change in coordination number. Therefore, in the next step, we probe the variation of mean coordination number of each species as a function of pressure using cutoff values of 2.61–2.90 Å for Zr–O and 2.14–2.35 Å for Si–O depending pressure. Fig. 4 illustrates the alteration of the average coordination of Zr, Si and O upon the compression and decompression processes. The average coordination number of Zr, Si and O at zero pressure is determined as ~5.7, 4.1 and 2.4, correspondingly. All mean coordination numbers alter almost in a similar manner, namely nonlinearly, under pressure. The coordination of Zr atoms is practically unaffected up to 6 GPa and quickly increases from 5.7 to 7.3 between 6.0 and 14 GPa. This coordination remains null in the range of 14 GPa–22 GPa. Above 23 GPa it starts to rise again, reaches a value of 8.0 at 29 GPa and residues constant up to 39 GPa. The change in Si coordination is almost similar to that in Zr coordination but its response to pressure arises at a slightly higher value. Such a behavior was also reported in Ref. [17] because Si–O bonds is stronger than Zr–O bonds [17]. Si coordination remains null until 9 GPa and rises from 4.1 to 4.9 between 9 GPa and 23 GPa. It reaches a value of 5.4 at 26 GPa and retains nearly constant up to 39 GPa. Upon decompression from 22 GPa (39 GPa), the coordination number is 6.7 (7.1) for Zr, 4.6 (5.0) for Si and 2.8 (3.0) for O. Note that these recovered coordination numbers are greater than the uncompressed values and Zr coordination in the recovered networks is quite comparable with around 7 in the metamict zircon [29–31]. On the other hand, it should be noted that the recovered structures have different Si coordination than the metamict zircon.

We perform the Voronoi polyhedra analysis to acquire additional information about the system at high pressure. A Voronoi polyhedron is expressed by the indices $< l_3,l_4,l_5,l_6, \ldots >$, where l_i and Σl_i are the number of i-edge faces of the polyhedron and its coordination number, respectively. In the zircon crystal, Zr atoms are represented by the <0,4,4,0> index. Such an index does not exist in the uncompressed network (see Fig. 5), suggesting no similarity between the amorphous and crystalline states. The uncompressed model largely consists of octahedrons and pentagons represented by <0,6,0,0> and <2,3,0,0> indices, respectively (see Fig. 6 obtained by the VESTA program [32]). As the pressure applied is slowly increased, the <0,4,4,0> type polyhedrons gradually develop and their fraction reaches 31% at 22 GPa and 50% at 39 GPa. We also notice the formation of sevenfold coordinated motifs having <0, 5,2,0> index, which is also observed in amorphous zirconia [26] and can be classified as an incomplete <0,4,4,0>-like motifs. The recovered amorphous configurations present similar type of polyhedrons as well. Additionally, ninefold coordinated clusters having <0,3,6,0> index and sevenfold coordinated polyhedrons with the <1,3,3,0> index are presented in these high pressure phases. Truly, they are the core building motifs of the cotunnite and baddaliyette crystals of zirconia, respectively. Therefore, on the basis of these outcomes, we recommend that the local structure of Zr-atoms in these amorphous states is partly related to that of Zr-atom in the crystal. The formation of the cotunnite type clusters might be an indication of a phase transformation into the cotunnite-like structure (amorphous or crystal) in the ZrO_2 domains at higher pressures.

Bond angle distribution functions (BADFs) of the amorphous zircon configuration under pressure are plotted in Fig. 7. We notice that all angles distribution functions show similar response to pressure. Namely their main peaks gradually shift to lower angles as expected due to the formation of high coordinated motifs. Noticeable peaks appear in the O–Si–O and the O–Zr–O bond angle distributions at high angles during pressurizing process and these high-pressure peaks are mainly preserved upon decompression.

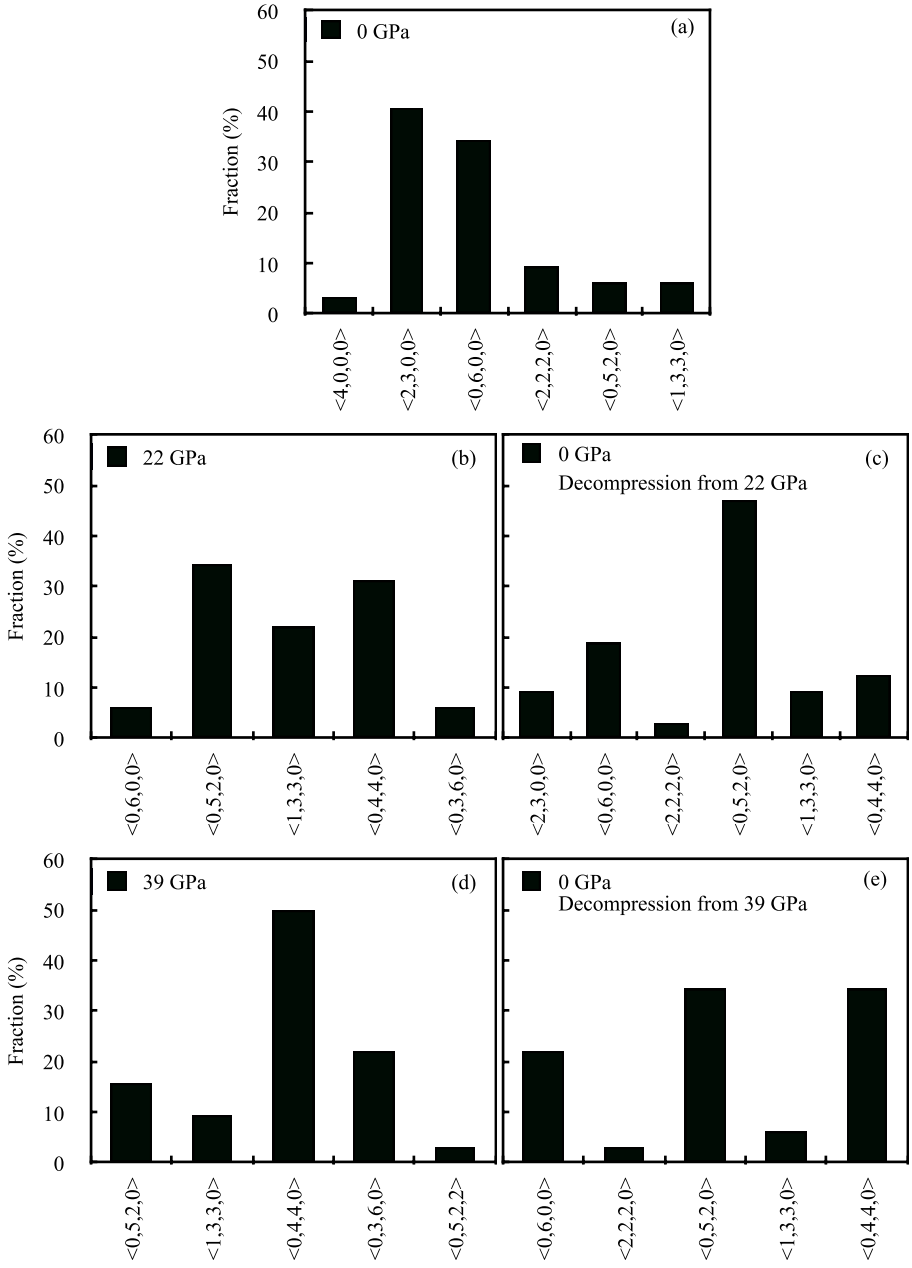

Fig. 5. Fraction of the Voronio polyhedrons at selected pressures.

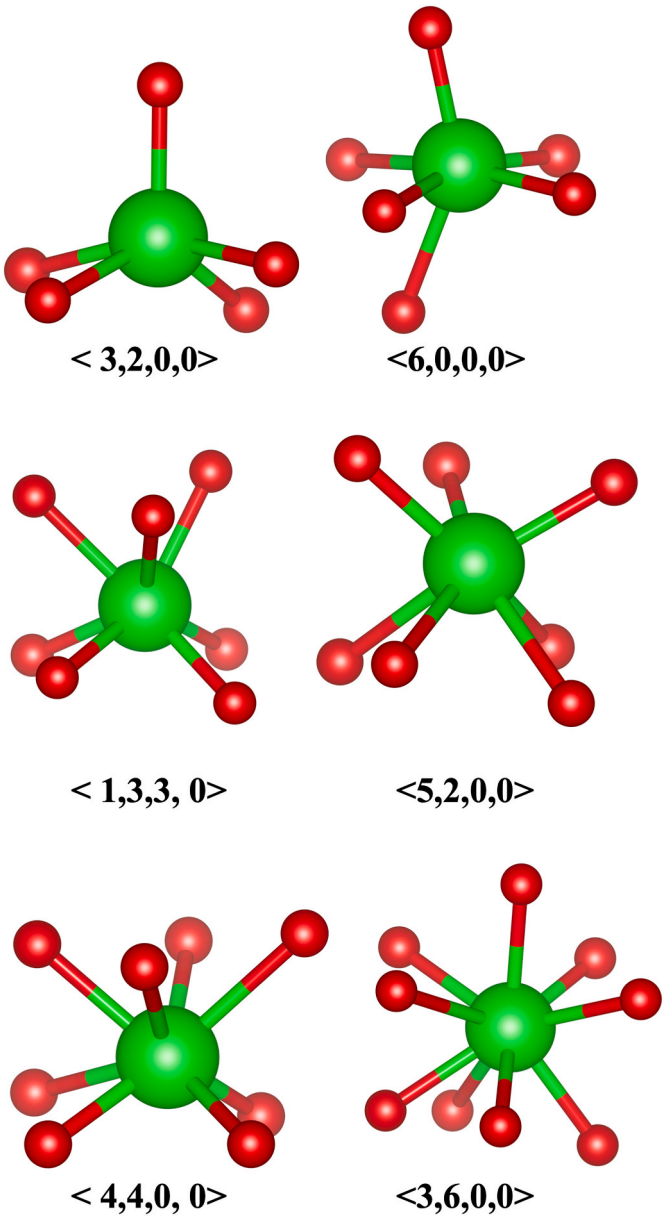

Fig. 6. The most common Voronio polyhedrons formed in amorphous zircon at ambient and high pressures.

4. Discussion

The structural evaluations unveil two potential amorphous-to-amorphous phase transformations in zircon. The first transformation occurs between 7 GPa and 15 GPa and involves a steady coordination modification of Zr (Si) atoms from 5.9 (4.1) to 7.3 (4.5). This phase remains stable up to 22 GPa. It should be noticed here that the coordination number of Zr atoms in this amorphous state is parallel to that of Zr atoms in the metamict zircon but Si atoms have a coordination number of 4.5, higher than the tetrahedral coordination in the metamict zircon. Therefore, this phase is moderately analogous to the metamict zircon. The second phase transformation happens between about 22 GPa and 27 GPa and involves a steady increase in Zr coordination from 7.3 to 8 and in Si coordination from 4.5 to 5.3. The coordination increase around Zr atoms is indeed similar to what has been observed in a joint experimental and theoretical study [17]. Consequently, the phase attained above 27 GPa is labelled as a HDA phase as in Ref. [17], but we do not know if the HDA phase observed in Ref. [17] is comparable with one proposed in the present work since the type of clusters formed at high pressures and information about Si coordination were not provided in details [17]. Based on the Voronoi polyhedra analysis, we claim that the HDA phase is rather comparable with the crystalline zircon and cotunnite like zirconia and at higher pressures the ZrO_2 domains can transform into the cotunnite-like structure.

It should be noted that with the application of pressure, Si-rich domains in our amorphous model act like SiO_2 glass in which Si coordination gradually changes from 4 to 6 between 18 and 40 GPa [33–35]. Yet a minor alteration in the pressure range where the transformation begins and completes and in Si coordination are observed in the present work. Since our model is a mixed state, such a difference is anticipated.

Upon decompression from two different pressures of 22 GPa and 39 GPa, a permeant densification is observed in this material, parallel to Refs. [17,18]. The recovered amorphous structures are partly related to the metamict zircon because their Zr coordination is comparable with that of the metamict zircon. Also depending on releasing pressures, different amorphous states are observed, similar to what has been proposed in Ref. [17]. All these findings and the results of Ref. [17] suggest that depending on the starting structures and decompression pressures, different transformation mechanisms can be achievable for amorphous zircon and there exist various amorphous forms of zircon having a different density and a local structure.

5. Conclusions

We study the pressure-induced modifications in a very low-density amorphous zircon configuration having Zr (Si) coordination of 5.6 (4.02) by means of ab initio simulations and propose possible two amorphous-to-amorphous phase transformations for this material. In the first phase change, a very low-density amorphous phase gradually converts to a dense amorphous state with Zr and Si coordination numbers of about 7.3 and 4.5, correspondingly. In this phase, ZrO_2 domains are partially similar to the metamict zircon and baddaliyette zirconia while the SiO_2 domains resemblance the densified silica glass. The second phase change is from the dense phase to a HDA phase with Zr and Si coordination numbers of about 8 and 5.5, respectively. In the HDA phase, the ZrO_2 domains are somewhat analogous to the metamict zircon and cotunnite zirconia. Both phase modifications proceed steadily. The first phase change is irreversible whist the second one is reversible.

CRediT authorship contribution statement

Süleyman Bolat: Investigation, Validation, Formal analysis, Data curation, Writing - original draft, preparation, Visualization. **Murat Durandurdu:** Conceptualization, Methodology, Resources, Supervision, Funding acquisition, Writing - review & editing.

Declaration of competing interest

The authors declare that they have no known competing financial interests or personal relationships that could have appeared to influence the work reported in this paper.

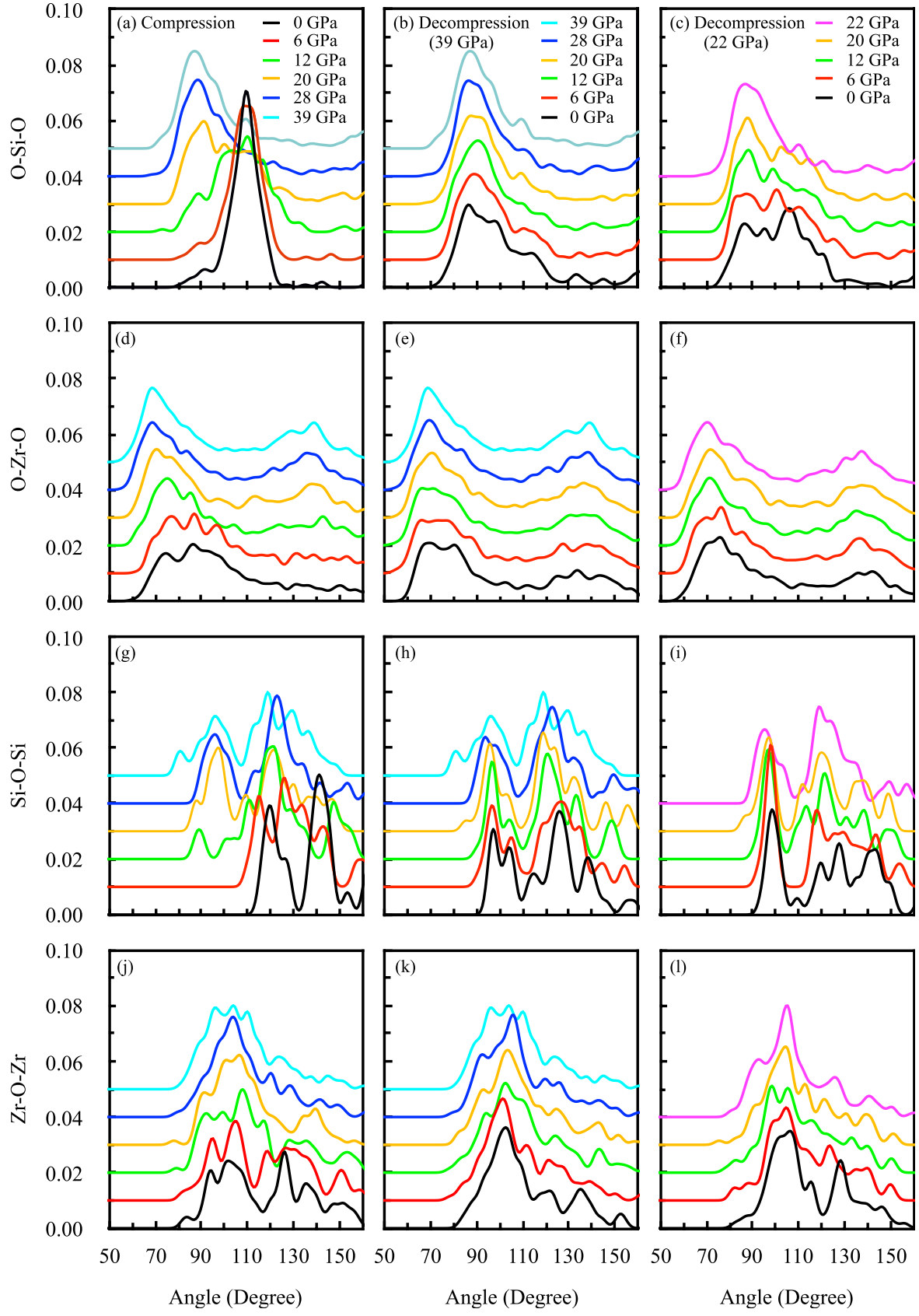

Fig. 7. Bond angle distribution functions (BADFs) of the amorphous zircon model at sellected pressures.

Acknowledgements

MD acknowledges financial support from the Abdullah Gül University support foundation. The calculations were run on TÜBİTAK ULAKBİM, High Performance and Grid Computing Center (TRUBA resources).

Appendix A. Supplementary data

Supplementary data to this article can be found online at https://doi.org/10.1016/j.jpcs.2021.109991.

References

[1] S.L. Chaplot, L. Pintschovius, N. Choudhury, R. Mittal, Phonon dispersion relations, phase transitions, and thermodynamic properties of ZrSiO4: inelastic neutron scattering experiments, shell model, and first-principles calculations, Phys. Rev. B 73 (1–8) (2006), 094308.
[2] R. Dutta, N. Mandal, Structure, elasticity and stability of reidite (ZrSiO4) under hydrostatic pressure: a density functional study, Mater. Chem. Phys. 135 (2012) 322–329.
[3] R.J. Finch, J.M. Hanchar, Structure and chemistry of zircon and zircon-group minerals, Rev. Mineral. Geochem. 53 (2003) 1–26.
[4] M.J. Akhtar, S. Waseem, Atomistic simulation studies of zircon, Chem. Phys. 274 (2001) 109–120.
[5] B.E. Burakov, E.B. Anderson, M.V. Zamoryanskaya, M.A. Yagovkina, E. E. Strykanova, Synthesis and study of 239Pu-doped ceramics based on zircon, (Zr, Pu)SiO4, and hafnon, (Hf,Pu)SiO4, in: Mater. Res. Soc., 2001, pp. 1–7.
[6] R.C. Ewing, Nuclear waste forms for actinides, in: Proc. Natl. Acad. Sci. U. S. A, 1999, pp. 3432–3439.
[7] X.Q. Cao, R. Vassen, D. Stoever, Ceramic materials for thermal barrier coatings, J. Eur. Ceram. Soc. 24 (2004) 1–10.
[8] B. Yang, B.J. Luff, P.D. Townsend, Cathodoluminescence of natural zircons, J. Phys. Condens. Matter 4 (1992) 5617–5624.
[9] K. Robinson, G.V. Gibbs, P.H. Ribbe, The structure of zircon: a comparison with garnet, Am. Mineral. 56 (1971) 782–790.
[10] R.M. Hazen, L.M. Finger, Crystal structure and compressibility of zircon at high pressure, Am. Mineral. 64 (1979) 196–201.
[11] A.F. Reid, A.E. Ringwood, Newly observed high pressure transformations in Mn3O4, CaAl2O4 and ZrSiO4, Earth Planet Sci. Lett. 6 (1969) 205–208.
[12] H.D. Holland, D. Gottfried, The effect of nuclear radiation on the structure of zircon, Acta Crystallogr. 8 (1955) 291–300.
[13] M.A. Russak, C.V. Jahnes, E.P. Katz, Reactive magnetron sputtered zirconium oxide and zirconium silicon oxide thin films, J. Vac. Sci. Technol. A Vacuum, Surfaces, Film. 7 (1989) 1248–1253.
[14] M. Nogami, Glass preparation of the ZrO2SiO2 system by the sol-gel process from metal alkoxides, J. Non-Cryst. Solids 69 (1985) 415–423.
[15] J. Du, R. Devanathan, L.R. Corrales, W.J. Weber, A.N. Cormack, Short- and medium-range structure of amorphous zircon from molecular dynamics simulations, Phys. Rev. B 74 (2006) 214204–214214.
[16] R. Devanathan, L.R. Corrales, W.J. Weber, A. Chartier, C. Meis, Molecular dynamics simulation of energetic uranium recoil damage in zircon, Mol. Simulat. 32 (2006) 1069–1077.
[17] K. Trachenko, V.V. Brazhkin, O.B. Tsiok, M.T. Dove, E.K.H. Salje, Pressure-induced structural transformation in radiation-amorphized zircon, Phys. Rev. Lett. 98 (2007) 135502–135504.
[18] F.A.P. Binvignat, Pressure - Induced Structural Changes in Metamict Zircon, 2015.
[19] S. Bolat, M. Durandurdu, Very low density amorphous phase of zircon, J. Non-Cryst. Solids 513 (2019) 137–143.
[20] D. Sánchez-Portal, P. Ordejón, E. Canadell, Daniel Sánchez-Portal, Pablo Ordejón, and Enric Canadell. "Computing the Properties of Materials from First Principles with SIESTA, Springer, Berlin, Heidelberg, 2004, pp. 103–170. Principles and Applications of Density Functional Theory in Inorganic Chemistry II. Springer, Berlin, Heidelberg, 2004. 1, in: Struct. Bond.
[21] N. Troullier, J.L. Martins, Efficient pseudopotentials for plane-wave calculations, Phys. Rev. B 43 (1993), 1993–2006.
[22] J.P. Perdew, K. Burke, M. Ernzerhof, Generalized gradient approximation made simple, Phys. Rev. Lett. 77 (1996) 3865–3868.
[23] L. Cartz, R. Fournelle, Metamict zircon formed by heavy ion bombardment, Radiat. Eff. 41 (1979) 211–217.
[24] M. Parrinello, A. Rahman, Polymorphic transitions in single crystals: a new molecular dynamics method, J. Appl. Phys. 52 (1981) 7182–7190.
[25] M. Durandurdu, Novel high-pressure phase of ZrO2: an ab initio prediction, J. Solid State Chem. 230 (2015) 233–236.
[26] M. Durandurdu, Amorphous zirconia at high pressure, J. Am. Ceram. Soc. 101 (2018) 5411–5418.
[27] E. Balan, F. Mauri, C.J. Pickard, I. Farnan, G. Calas, The aperiodic states of zircon: an ab initio molecular dynamics study, Am. Mineral. 88 (2003) 1769–1777.
[28] R. Devanathan, L.R. Corrales, W.J. Weber, A. Chartier, C. Meis, Molecular dynamics simulation of disordered zircon, Phys. Rev. B 69 (2004), 064115–9.
[29] F. Farges, The structure of metamict zircon: a temperature-dependent EXAFS study, Phys. Chem. Miner. 20 (1994) 504–514.
[30] R.C. Ewing, A. Meldrum, L.M. Wang, W.J. Weber, L.R. Corrales, Radiation effects in zircon, Rev. Mineral. Geochem. 53 (2003) 387–425.
[31] I. Nakai, J. Akimoto, M. Imafuku, R. Miyawaki, Y. Sugitani, K. Koto, Characterization of the amorphous state in metamict silicates and niobates by EXAFS and XANES analyses, Phys. Chem. Miner. 15 (1987) 113–124.
[32] K. Momma, F. Izumi, VESTA 3 for three-dimensional visualization of crystal, volumetric and morphology data, J. Appl. Crystallogr. 44 (2011) 1272–1276.
[33] T. Sato, N. Funamori, High-pressure structural transformation of SiO2 glass up to 100 GPa, Phys. Rev. B 82 (2010), 184102–5.
[34] C.J. Benmore, E. Soignard, S.A. Amin, M. Guthrie, S.D. Shastri, P.L. Lee, J. L. Yarger, Structural and topological changes in silica glass at pressure, Phys. Rev. B 81 (2010), 054105–5.
[35] A. Zeidler, K. Wezka, R.F. Rowlands, D.A.J. Whittaker, P.S. Salmon, A. Polidori, J. W.E. Drewitt, S. Klotz, H.E. Fischer, M.C. Wilding, C.L. Bull, M.G. Tucker, M. Wilson, High-pressure transformation of SiO2 glass from a tetrahedral to an octahedral network: a joint approach using neutron diffraction and molecular dynamics, Phys. Rev. Lett. 113 (2014) 135501–135505.